Assessment of Arctic Sea Ice and Surface Climate Conditions in Nine CMIP6 Climate Models

Enter authors here: Martin Henke[1], Celso M. Ferreira[1],Jinlun Zhang[2], Thomas M. Ravens[3], Tyler Miesse[1], Felício Cassalho[1]

[1] Department of Civil, Environmental, and Infrastructure Engineering, George Mason University, Fairfax, VA,

[2] Polar Science Center, Applied Physics Laboratory, University of Washington, Seattle, WA, USA.

[3] College of Engineering, University of Alaska Anchorage, Anchorage, AK, USA

Corresponding author: Martin Henke (mhenke@gmu.edu)

Key Points:

- Climate Models participating in Coupled Model Intercomparison Project Phase 6 are assessed for historical simulation of Arctic sea ice.
- Model sea ice thickness simulation accuracy varies considerably seasonally between months and spatially between regions.
- Most models fail to simulate the thickest regions of sea ice and possess a positive bias over the Eurasian Shelf.

Abstract

The observed retreat and anticipated further decline in Arctic sea ice holds strong climate, environmental, and societal implications. In predicting climate evolution, ensembles of coupled climate models have demonstrated appreciable accuracy in simulating sea ice area and volume trends throughout the historical period. However, individual climate models still show significant differences in simulating the sea ice thickness distribution. To better understand individual model performance in sea ice simulation, nine climate models previously identified to provide plausible sea ice decline and global temperature change were evaluated in comparison with Arctic satellite and reanalysis derived sea ice thickness data, sea ice extent records, and atmospheric reanalysis data of surface wind and air temperature. Assessment found that the simulated spatial distribution of historical sea ice thickness varies greatly between models and that several key limitations persist among models. Primarily, most models do not capture the thickest regimes of multi-year ice present in the Wandel and Lincoln Seas; those that do, often possess erroneous positive bias in other regions such as the Laptev Sea or along the Eurasian Arctic Shelf. From analysis, no model could be identified as performing best overall in simulating historic sea ice, as model bias varies regionally and seasonally. Nonetheless, the bias maps and statistical measures derived from this analysis should enhance understanding of the limitations of each climate model. This research is motivated in-part to inform future usage of coupled climate model projection for regional modeling efforts and enhance climate change preparedness and resilience in the Arctic.

Plain Language Summary

The expected future decline in Arctic sea ice will have far-reaching global impacts. In simulating sea ice, many global climate models have shown skill in predicting the seasonal cycle and area of sea ice, yet struggle in simulating sea ice thickness. This study evaluates the ability of nine climate models to simulate sea ice thickness in different Arctic regions and months. This is accomplished by comparing historical climate model simulations to reference data such as satellite observations. Additionally, model simulations of sea ice extent and climate variables related to sea ice dynamics (surface wind speed and air temperature) are assessed to provide insight into related and driving variables. From this process, we found that while sea ice thickness varies substantially between models, there are some common areas that models struggle to simulate. Namely, sea ice thickness is often too thin in the Wandel and Lincoln Seas, and too thick in the Laptev Sea or along the Eurasian Arctic Shelf. No single model is identified as best due to changing performance depending on season and region. However, this analysis should give insight of model performance for those interested in utilizing climate model simulations for predicting climate change in the Arctic.

1 Introduction

Arctic sea ice has declined dramatically over the previous century, foremost demonstrated by a persistent negative trend in sea ice area from 1979 to the present (Doscher et al., 2014; Laxon et al., 2013; Julienne Stroeve & Notz, 2018). Thinning of sea ice regimes has also been confirmed, as the prevalence of perennial multi-year ice has diminished, being replaced by seasonal first-year ice (Kwok, 2018; Maslanik et al., 2007; Julienne Stroeve & Notz, 2018). This first-year sea ice is: i) thinner than perennial sea ice (Tschudi et al., 2016), ii) more

dynamic (Kwok et al., 2013; Olason & Notz, 2014), and iii) further responsive to atmospheric and oceanic forcing (Kwok, 2018; Overland, 2020). Sea ice plays a critical role in Arctic atmosphere and ocean processes; modifying the thermal energy budget through high surface albedo and suppressing air-sea heat, moisture, and momentum fluxes (Mercè Casas-Prat & Wang, 2020; Goosse et al., 2018; Haine et al., 2015; Karlsson & Svensson, 2013; Mioduszewski et al., 2018; Julienne Stroeve & Notz, 2018; Thomson & Rogers, 2014; Timmermans & Marshall, 2020). Beyond geophysical effects, reduced Arctic sea ice cover is anticipated to have considerable societal effects with potential increases in Arctic maritime activity (Aksenov et al., 2017; Chen et al., 2020; Sibul & Jin, 2021), growing regional development (Harsem et al., 2015), and greater risk of coastal hazards to impact Arctic communities (Barnhart et al., 2014; Mioduszewski et al., 2018; Williams & Erikson, 2021). As the reality of an "ice-free" summer (sea ice area less than 1×106 km2) is predicted to occur before 2050 (Chen et al., 2020; SIMIP Community, 2020; Wei et al., 2020), accurate forecasting of sea ice is crucial to facilitate understanding and preparedness for future impacts.

Climate models participating in the Coupled Model Intercomparison Project's sixth phase (CMIP6) have shown marked improvement in simulating sea ice cover in comparison to prior phases. The multimodel mean of sea ice extent (SIE) generally captures the seasonal amplitude between March peak SIE and the September low. Yet, most models underestimate the observed downward trend of sea ice extent, and there is a wide intermodel spread during the summer months when the greatest negative trend occurs (Long et al., 2021; Shen et al., 2021; Shu et al., 2020; SIMIP Community, 2020). Even models shown to best follow the observed seasonal sea ice area and volume still experience numerous challenges in simulating the spatial distribution of sea ice thickness (Davy & Outten, 2020; Watts et al., 2021).

This research seeks to assess CMIP6 climate models' skill in simulating historic sea ice thickness, extent, and related surface climate variables in order to identify potential candidates for future dynamic downscaling. Intensive effort has been directed towards analyzing CMIP6 models' sea ice cover simulation in the interest of improving climate projection (Shen et al., 2021; Shu et al., 2020; SIMIP Community, 2020; Watts et al., 2021). Accurate forecasts of sea ice are crucial to Arctic stakeholders impacted by changing sea ice conditions and dependent Arctic research efforts such as wave projections (M. Casas-Prat et al., 2018) or arctic maritime accessibility studies (Chen et al., 2020; Melia et al., 2016). By enhancing understanding of model simulation of sea ice and related surface climate variables (wind speed and surface air temperature), this research is intended to provide a resource for future Arctic research reliant on the accuracy of climate model projections. It should be recognized that accurate simulation of historic conditions does not guarantee future projection accuracy. However, the inverse, consistent bias in simulating historical conditions does imply model shortcomings, and thus the process of model selection using historical performance criteria is necessary and has been shown to significantly influence the trajectory of future projections (Docquier & Koenigk, 2021; Knutti et al., 2017).

To assess model simulation, historic Arctic sea ice and related surface climate variables were evaluated from the beginning of the satellite era to the end of the CMIP6 historical experiment (1979-2014). The sea ice variables assessed included sea ice thickness (SIT) and sea ice extent (SIE), and the surface climate variables assessed included surface wind speed (SWS) and surface air temperature (SAT). SWS and SAT were selected for analysis because they are important sea ice drivers and have Pan-Arctic availability and reasonable accuracy from

atmospheric reanalysis products. These variables were compared monthly with remote sensing derived data, reanalysis sea ice products, and atmospheric reanalysis products. SIT simulation was evaluated in comparison to both the Pan-Arctic Ice Ocean Modeling and Assimilation System (PIOMAS) sea ice thickness reanalysis and merged CryoSat-2-SMOS sea ice thickness measurements 2011- 2014. The National Snow and Ice Data Center (NSIDC) Sea Ice Index (SII) was used to assess model simulation of average monthly SIE and trends. Finally, ERA5 atmospheric reanalysis was used in assessing model simulation of both SAT and SWS variables. Supplementing the Pan-Arctic analysis, model simulation of SIT within the Canadian Archipelago and the nearby Baffin Bay was analyzed.

2 Data and Methods

2.1 Model Selection

Models selected for evaluation were identified from a previous assessment that identified models which forecast a realistic amount of sea ice loss while concurrently simulating a plausible global mean temperature change (SIMIP Community, 2020). The nominal horizontal resolution of the analyzed climate models differs substantially. Model resolution has been found to influence the accuracy of models, with higher resolution models tending to exhibit better simulation of oceanic heat transfer (Docquier et al., 2019). The CMIP6 historical experiment provides historical simulation data in varying temporal resolution; in this research, monthly averages of simulated variables were assessed. Multiple simulation realizations are available for all but two of the models evaluated as shown in Table 1. These two models: CNRM-CM6-1-HR and GFDL-ESM4, have only one available realization member, and thus robust conclusions pertaining to either model's physics are indeterminate. However, this does not negate the performance of the individual realization.

Table 1. Climate models evaluated within the study, individual ocean grid resolution, affiliated institution, and the number of ensemble members available/used.

Climate Model	Sea Ice Grid Resolution	Institution ID	Ensemble Members
ACCESS-CM2	360 × 300	CSIRO-ARCCSS	5
CESM2-WACCM	384 × 324	NCAR	3
CNRM-CM6-1-HR	1442 × 1050	CNRM-CERFACS	1
GFDL-ESM4	720 × 576	NOAA-GFDL	1
GISS-E2-2-G	90 × 144	NASA-GISS	10
MPI-ESM-1-2-HAM	256 × 220	MPI-M	3
MPI-ESM-1-2-HR	404 × 802	HAMMOZ-Consortium	10
MRI-ESM2-0	363 × 360	MRI	10
NorESM2-MM	360 × 384	NCC	3

2.2 Sea Ice Evaluation

SIT accuracy is assessed through comparison with the Alfred Wegner Institute's combined CryoSat-SMOS (CS2SMOS) Merged Sea Ice Thickness data product (Ricker et al., 2017) and PIOMAS sea ice reanalysis dataset. The merged satellite data product utilizes both CryoSat-2 and SMOS derived SIT measurements. The combined analysis SIT product is

enhanced to measure a greater range of sea ice thickness regimes – most notably thin ice from SMOS (Kwok & Cunningham, 2015; X. Wang et al., 2016). The CS2SMOS SIT product provides monthly coverage from October through April. However, full monthly data for October and April is incomplete, with the dataset beginning in late October and terminating in early April; this may potentially introduce a positive and negative bias for both monthly means respectively. The overlap between complete CS2SMOS data and the CMIP6 historical experiment begins in 2011 and ends in 2014. Given the brevity in this period of assessment, and the inclusion of 2012 – the anomaly lowest summer SIE on record - an additional basis of assessment was needed to evaluate the mean distribution of sea ice. For this purpose, the Pan-Arctic Ice Ocean Modeling and Assimilation System (PIOMAS) sea ice thickness reanalysis is used for SIT comparison monthly 1979 – 2014 (A. Schweiger et al., 2011; Zhang & Rothrock, 2003). PIOMAS provides monthly full-year coverage and allows for the annual sea ice minimum occurring in September to be analyzed.

The process of model SIT comparison is described as follows: i) the average was taken across ensemble members, ii) monthly sea ice grids were linearly interpolated onto either the CS2SMOS or PIOMAS grid, iii) months were averaged across the entire analysis period establishing a month SIT mean, and iv) model and reference grids were subtracted to create error maps and derive statistical measures. Grid cells where both model and reference agree on open water conditions were excluded from the derivation of statistical measures to reduce the effect of large open water areas during summer months. Following Pan-Arctic analysis, regional analysis for the Canadian Archipelago was performed, and summary statistics were derived for the area. Regional analysis limits analysis to the coordinates between latitudes 60°N to 80°N and longitudes 50°W to 130°W which effectively encompasses the Canadian Archipelago and Baffin Bay.

Evaluation of climate model SIE is assessed with monthly SIE values reported from the NSIDC's Sea Ice Index (Meier et al., 2017; Peng et al., 2013). Arctic SIE is defined as the total Arctic area possessing a minimum of 15% sea ice concentration (SIC). Each model's native grid was used to derive SIE, then the average of all realizations was taken to create the ensemble mean SIE time series. These values are then compared with the NSIDC Sea Ice Index value to determine bias.

2.3 Surface Climate Evaluation

The European Center for Medium Range Forecasts' ERA5 atmospheric reanalysis provides reference for SAT and SWS simulation analysis. Both surface air temperature and surface wind speed were analyzed in comparison to ERA5 historical atmospheric climate reanalysis data product. In a study of atmospheric reanalysis products within the Arctic, ERA5 or ERA-interim (predecessor to ERA5) simulated SAT and SWS were found to have high correlation and low error in comparison to the observed Arctic surface climate, thus qualifying the reanalysis for use in comparison (Demchev et al., 2020; Graham et al., 2019; Lindsay et al., 2014). However, it should be noted that ERA5 possesses a warm bias under extremely cold winter conditions (Davy & Outten, 2020; Demchev et al., 2020; Graham et al., 2019; C. Wang et al., 2019).

3 Results

3.1 Sea Ice Thickness

The European Center for Medium Range Forecasts' ERA5 atmospheric reanalysis provides reference for SAT and SWS simulation analysis. Both surface air temperature and surface wind speed were analyzed in comparison to ERA5 historical atmospheric climate reanalysis data product. In a study of atmospheric reanalysis products within the Arctic, ERA5 or ERA-interim (predecessor to ERA5) simulated SAT and SWS were found to have high correlation and low error in comparison to the observed Arctic surface climate, thus qualifying the reanalysis for use in comparison (Demchev et al., 2020; Graham et al., 2019; Lindsay et al., 2014). However, it should be noted that ERA5 possesses a warm bias under extremely cold winter conditions (Davy & Outten, 2020; Demchev et al., 2020; Graham et al., 2019; C. Wang et al., 2019).

Comparison of model-simulated monthly SIT and averaged CS2SMOS observations for October and March over the four-year period 2011-2014 yields bias plots for October (Fig. 1a) and March (Fig. 1b). The summary statistics for both months are presented in Table 2 along with the overall statistics averaged over October through April. CS2SMOS data is unavailable for the annual sea ice minimum month (September) and does not start until the latter half of the month of October. This potentially introduces a positive SIT bias into the month's average used for comparison. Despite this, over half the models exhibit a positive bias for October, ranging from 16cm to over 1m. For most models, this stems from an erroneous region of thick sea ice in Eastern Siberian and Chukchi Seas, most pronounced in the ACCESS-CM2, CESM2-WACCM, MPI-ESM-1-2-HAM, and NorESM2-MM models. This phenomenon has been previously observed as common to the majority of CMIP5 models analyzed (J. Stroeve et al., 2014), and it is notable that several models do not possess this feature. The three models with the highest mean positive bias for October are CESM2-WACCM, MPI-ESM-1-2-HAM, and NorESM2-MM having mean bias values of 0.31m, 0.44m, 1.06m respectively. CESM2-WACCM incorrectly calculates a region of very thick ice (>2m) at the outer edge of the sea ice areas for October. It also simulates extremely thick ice (>6m) at several locations within the Canadian Archipelago. MPI-ESM-1-2-HAM shows positive bias (>1m) near the Laptev Sea and NorESM2-MM model has significant positive bias throughout the Arctic.

Previous climate model evaluations have shown models typically underestimate especially thick sea ice regimes. This holds true with the majority of models evaluated which undercalculated the thick multi-year ice observed at the Wandel Sea, Lincoln Sea, and north of the Canadian Archipelago. CESM2-WACCM is able to simulate part of the sea ice regime occurring along the northern coast of Greenland; yet it underestimates the continuation of the field towards the pole. MPI-ESM-1-2-HAM shows only slight underestimation (≈ -0.5m) of the thickest sea ice region during October, with bias growing into March. The only model to overrepresent ice in this region is the NorESM2-MM model, which shows significant positive bias throughout the Arctic. Recent research has shown the multi-year ice dominant in this region is more vulnerable to climate change than previously thought (A. J. Schweiger et al., 2021), and thus may be more responsive to climatic forcing (Overland, 2020). In March, nearly all models show improved spatial correlation in comparison to October – as models typically struggle to capture the annual sea ice minimum. Conversely, GISS-E2-1-G spatial correlation drops significantly from 0.72 to 0.51 from October to March; this is primarily attributed to significant

overestimation of March sea ice area far into southern Bering Sea and extending into the Pacific Ocean. All models show positive bias of varying magnitude and extent in the Laptev Sea and commonly extending into the Eastern Siberian Sea. Models maintaining a correlation of $r \geq 0.8$ overall are CNRM-CM6-1-HR, GFDL-ESM4, MPI-ESM-1-2-HAM, and MPI-ESM-1-2-HR. Of these, MPI-ESM-1-2-HR shows the lowest mean bias and the highest correlation coefficient.

Table 2. Statistics of error between each model's ensemble average and the reference CS2SMOS Analysis SIT for the individual months of October and March; and an average of winter months (October through April) 2011 to 2014. RMSE and Mean Bias have a unit of meters.

MODEL	ACCESS-CM2	CESM2-WACCM	CNRM-CM6-1-HR	GFDL-ESM4	GISS-E2-1-G	MPI-ESM-1-2-HAM	MPI-ESM-1-2-HR	MRI-ESM2-0	NorESM 2-MM
OCTOBER									
RMSE	0.62	0.93	0.68	0.52	**0.35**	0.72	0.46	0.53	1.41
MEAN BIAS	0.27	0.31	-0.34	-0.19	0.17	0.44	**-0.09**	-0.10	1.06
R	0.66	0.28	0.77	0.80	0.72	0.72	**0.85**	0.74	0.65
MARCH									
RMSE	0.68	0.77	0.57	0.57	0.90	0.66	**0.55**	0.58	1.16
MEAN BIAS	0.34	0.22	-0.13	-0.09	0.66	0.29	**0.08**	**0.08**	0.80
R	0.79	0.67	**0.83**	0.81	0.51	**0.83**	0.82	0.79	0.76
AVERAGE (OCT – APR)									
RMSE	0.64	0.76	0.58	0.53	0.72	0.64	**0.51**	0.54	1.18
MEAN BIAS	0.28	0.15	-0.20	-0.12	0.48	0.30	**0.01**	-0.03	0.81
R	0.77	0.61	0.80	0.80	0.54	0.81	**0.82**	0.78	0.74

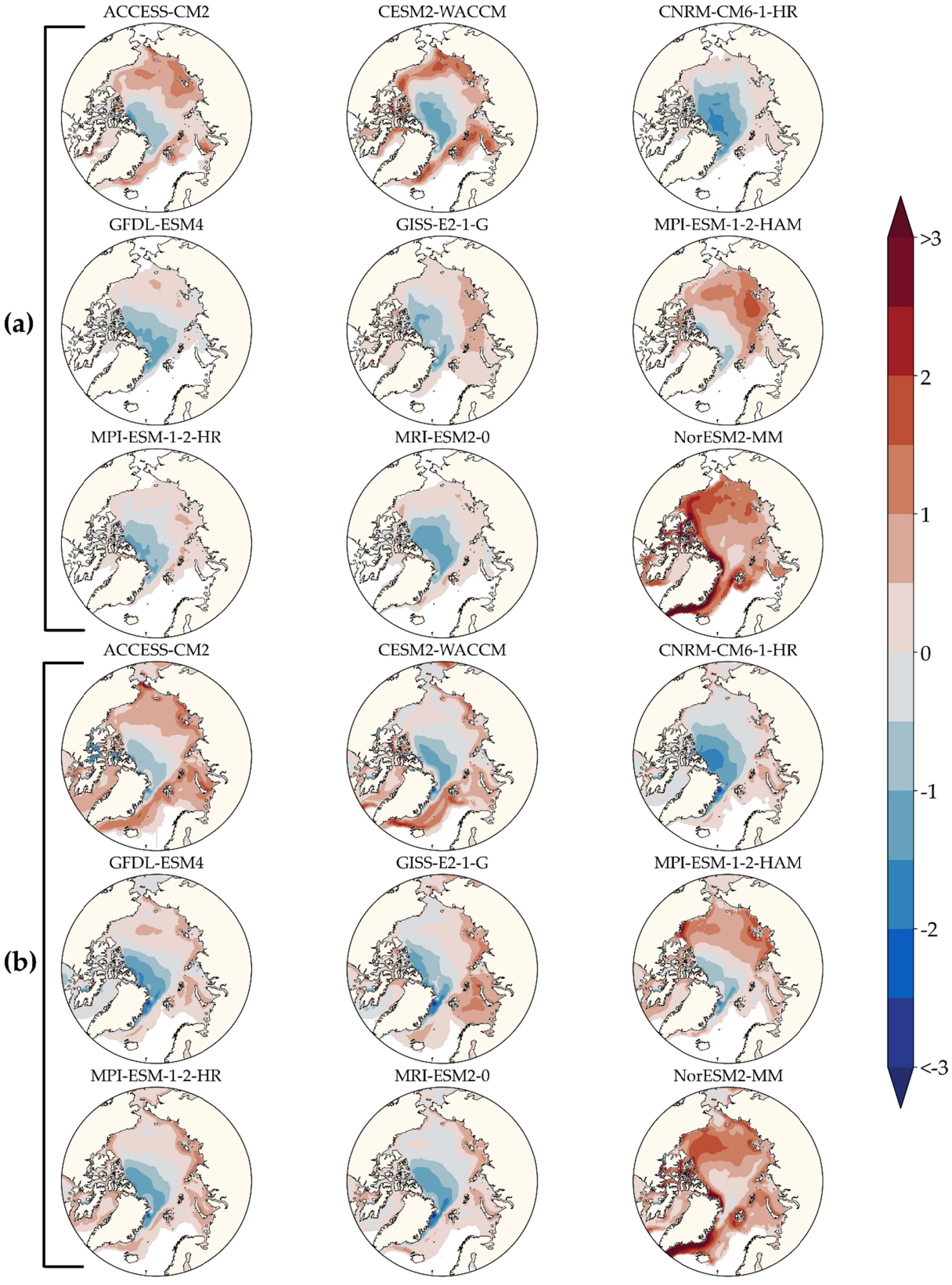
(a)
ACCESS-CM2
CESM2-WACCM
CNRM-CM6-1-HR
GFDL-ESM4
GISS-E2-1-G
MPI-ESM-1-2-HAM
MPI-ESM-1-2-HR
MRI-ESM2-0
NorESM2-MM
(b)
ACCESS-CM2
CESM2-WACCM
CNRM-CM6-1-HR
GFDL-ESM4
GISS-E2-1-G
MPI-ESM-1-2-HAM
MPI-ESM-1-2-HR
MRI-ESM2-0
NorESM2-MM
>3
2
1
0
-1
-2
<-3

Figure 1. Sea ice thickness bias (meters) between model ensemble mean and CS2SMOS for October (a) and March (b), over the period 2011-2014.

Supplementing the comparison via CS2SMOS data, climate models were evaluated using the extended PIOMAS sea ice reanalysis 1979 – 2014. Differing in this step of assessment – September monthly averages are compared rather than October used for CS2SMOS. Almost all models show increased agreement with PIOMAS; suspected drivers of this result include the lengthened time series, and the fact that PIOMAS itself exhibits bias in several regions common to climate models including the aforementioned positive bias in the Eastern Siberian and Chukchi seas (J. Stroeve et al., 2014). Three models (ACCESS-CM2, CESM2-WACCM, MPI-ESM-1-2-HAM) simulate the thick sea ice north of Greenland with negative bias less than >1m in both March and September; all other models underpredict SIT in this region with exception of NorESM2-MM possessing a Pan-Arctic positive bias. Similar to the CS2SMOS comparison for October, CESM2-WACCM again has erroneous high SIT at the outer edge of September Sea ice area which drives low correlation and high bias. While MPI-ESM-1-2-HR performed best in comparison to CS2SMOS overall, MPI-ESM-1-2-HAM and GISS-E2-1-G perform markedly better in comparisons to PIOMAS. The improved correlation of GISS-E2-1-G is notable, as this model exhibited the lowest correlation with CS2SMOS data. Further inspection into this result shows that this model exhibits negative bias in comparison to PIOMAS and large positive bias in comparison to the CS2SMOS data; suggesting that the model may not capture the thinning of sea ice regimes in later years.

Table 3. Statistics of error between each model's ensemble average and the reference PIOMAS reanalysis SIT for the individual months of September and March; and an average of all months 1979 through 2014. RMSE and Mean Bias have a unit of meters.

MODEL	ACCESS-CM2	CESM2-WACCM	CNRM-CM6-1-HR	GFDL-ESM4	GISS-E2-1-G	MPI-ESM-1-2-HAM	MPI-ESM-1-2-HR	MRI-ESM2-0	NorESM 2-MM
SEPTEMBER									
RMSE	1.04	1.57	1.02	0.90	0.68	0.66	**0.64**	0.70	2.01
MEAN BIAS	0.68	1.05	-0.68	-0.59	-0.30	0.31	-0.30	**0.07**	1.65
R	0.72	0.45	0.82	0.75	**0.87**	0.84	**0.87**	0.76	0.67
MARCH									
RMSE	0.76	0.89	0.93	0.84	0.67	**0.60**	0.67	0.69	1.31
MEAN BIAS	0.27	0.15	-0.60	-0.53	-0.23	**0.01**	-0.24	-0.42	0.77
R	0.83	0.73	0.87	0.86	0.89	0.87	0.88	**0.93**	0.78
ANNUAL									
RMSE	0.91	1.13	0.96	0.83	0.66	**0.60**	0.65	0.73	1.61
MEAN BIAS	0.46	0.44	-0.63	-0.51	-0.23	**0.12**	-0.24	-0.21	1.11
R	0.78	0.62	0.85	0.84	**0.89**	0.87	0.87	0.82	0.73

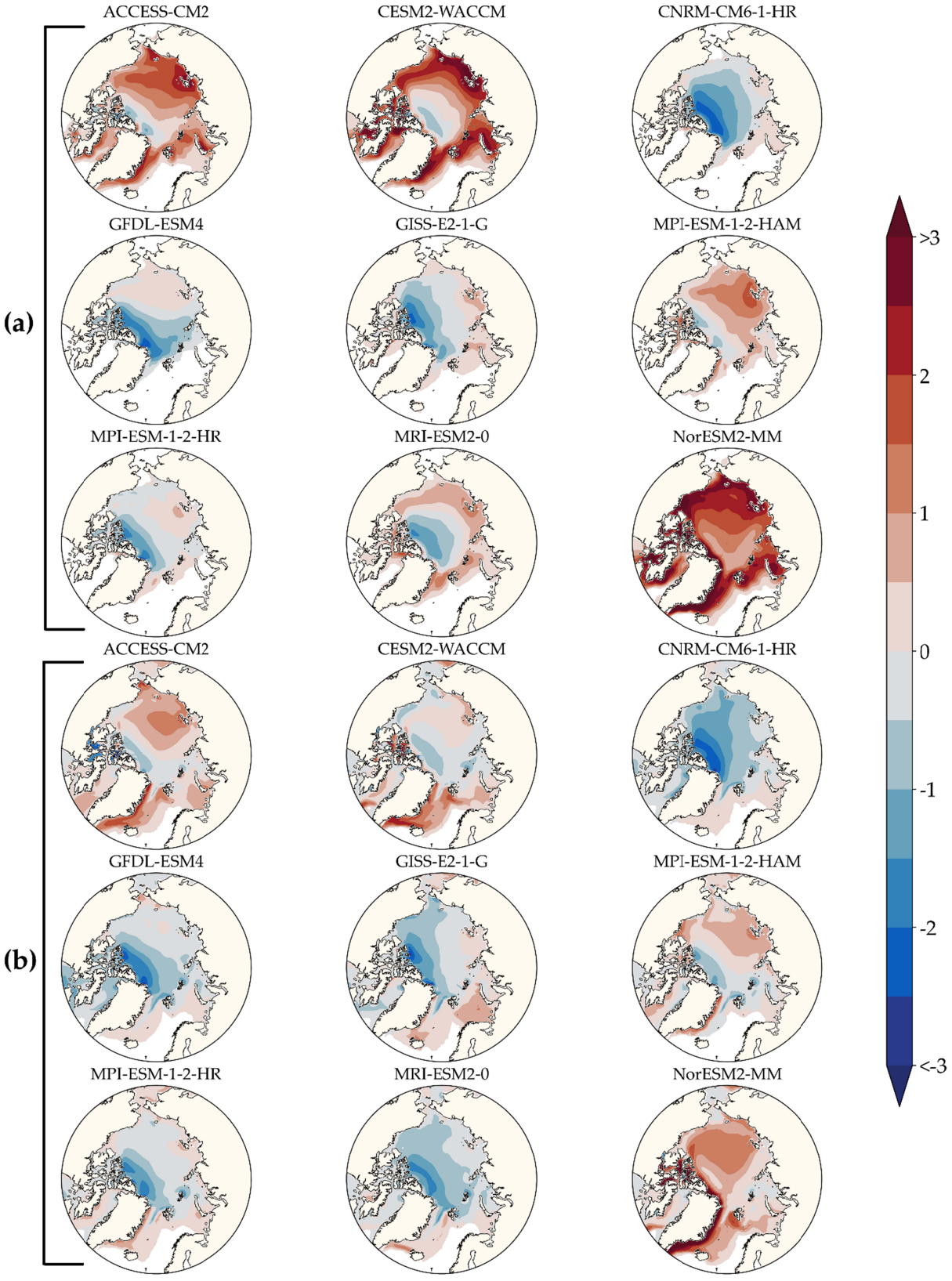
(a)
ACCESS-CM2
CESM2-WACCM
CNRM-CM6-1-HR
GFDL-ESM4
GISS-E2-1-G
MPI-ESM-1-2-HAM
MPI-ESM-1-2-HR
MRI-ESM2-0
NorESM2-MM
(b)
ACCESS-CM2
CESM2-WACCM
CNRM-CM6-1-HR
GFDL-ESM4
GISS-E2-1-G
MPI-ESM-1-2-HAM
MPI-ESM-1-2-HR
MRI-ESM2-0
NorESM2-MM
>3
2
1
0
-1
-2
<-3

259

Figure 2. Sea ice thickness bias (meters) between model ensemble mean and PIOMAS for October (a) and March (b), over the period 2011-2014.

3.2 Canadian Archipeligo Sea Ice Thickness

CMIP6 climate models have demonstrated positive biases for SIT within the Canadian Archipelago (Davy & Outten, 2020). Investigating the performance of individual models in this region is relevant to understanding future development and maritime travel along Arctic sea routes such as the Northwest Passage. Analysis we performed in comparison to PIOMAS and the localized summary statistics in this area defined by latitudes 60°N to 80°N and longitudes 50°W to 130°W can be seen in Table 3. CNRM-CM6-1-HR, GFDL-ESM4, GISS-E2-1-G, and MPI-ESM-1-2-HAM models have correlation coefficient $r \geq 0.8$, with MPI-ESM-1-2-HAM having the lowest RMSE (as it did for the pan-Arctic assessment). The majority of models show positive bias through most of the Canadian Archipelago, yet the three models with highest resolution (CNRM-CM6-1-HR, GFDL-ESM4, MPI-ESM-1-2-HR) trend toward negative bias for most of the region. These three models have similar SIT spatial distributions as seen in Figure 3 and possess strong negative bias in the Queen Elizabeth Islands in the northern part of the archipelago. GISS-E2-1-G trends toward overestimation of SIT throughout the region with several isolated locations of intense SIT along the western part of Baffin Bay. As the model with coarsest spatial resolution, GISS-E2-1-G's high correlation coefficient, comparable to that of the high-resolution models (CNRM-CM6-1-HR, MPI-ESM-1-2-HR) is unexpected – as model resolution would be expected to be a key factor in simulating sea ice dynamics within the region (Docquier et al., 2019). Within the northern part of the Canadian Archipelago, CESM2-WACCM simulates localized extreme SIT values exceeding 10 meters; this in part drives the poor spatial correlation and high error statistics for this model. By applying a SIT cutoff at 6m (such as that applied by Watts et al. (Watts et al., 2021)) the model performance is improved markedly, as the correlation coefficient rises to 0.52 while RMSE and mean bias fall to 1.3m and 44cm respectively.

Table 4. Regional Summary statistics of error for the Canadian Archipelago and Baffin Bay between each climate model and the reference PIOMAS SIT compared September 1979 - 2014. Mean, and RMSE have a unit of meters.

MODEL	ACCESS-CM2	CESM2-WACCM	CNRM-CM6-1-HR	GFDL-ESM4	GISS-E2-1-G	MPI-ESM-1-2-HAM	MPI-ESM-1-2-HR	MRI-ESM2-0	NorESM 2-MM
SEPTEMBER									
RMSE	0.93	1.70	0.90	0.98	0.72	**0.62**	0.74	0.69	1.81
MEAN BIAS	**-0.01**	0.53	-0.62	-0.75	-0.29	-0.07	-0.34	-0.09	0.95
R	0.61	0.45	0.80	0.80	0.80	**0.82**	0.78	0.77	0.64

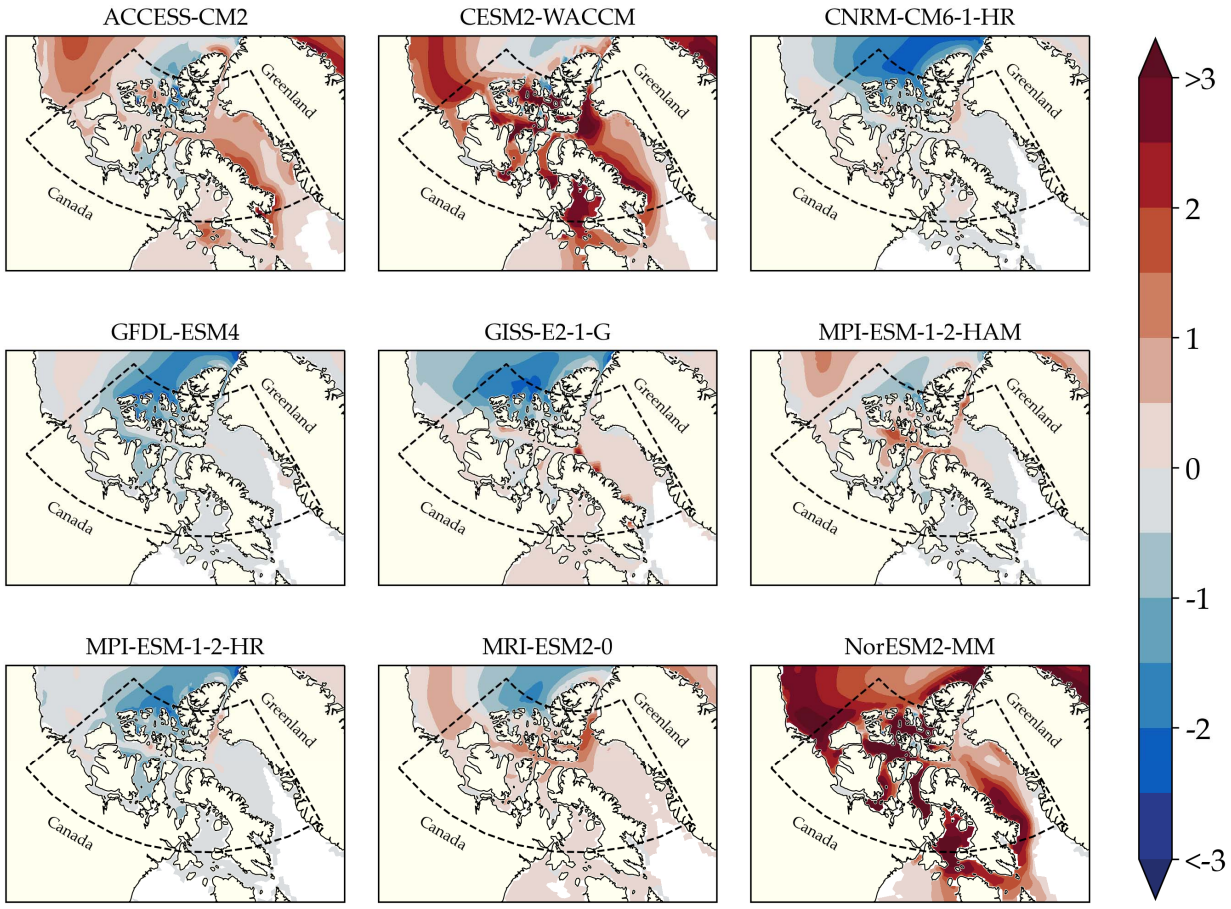

Figure 3. Sea ice thickness bias (meters) between model ensemble mean and PIOMAS for September within the Canadian Archipelago 1979 -2014. The delineation boundary is shown for selection of data used in deriving statistical measures.

3.3 Sea Ice Extent

Sea ice coverage within the Arctic is a critical parameter in governing Arctic surface exchange of heat, mass, and momentum and thus has been the topic of several CMIP6 and CMIP5 studies (Shen et al., 2021; Shu et al., 2020). The current generation of CMIP6 climate models typically over-represent SIE during both the seasonal maximum during March and the annual minimum during September (Shu et al., 2020). In this analysis, the majority of models overpredict SIE in summer months, yet are more evenly distributed during winter months as seen in Figure 4. One model, GISS-E2-1-G, shows considerably large positive bias throughout the year and peaking in March. CESM2-WACCM, GFDL-ESM4, CNRM-CM6-1-HR and MPI-ESM-1-2-HR have a mean absolute percentage error less than 4% annually and for September. These same models have the lowest September percent error among all models. GFDL-ESM4 and MPI-ESM-1-2-HR are closest to the mean September SIE area, with 1% and -1% percent error respectively. The observed and simulated linear trends in SIE loss for the month of September 1979 - 2014 is shown in Figure 4b and corresponding statistics are provided in Table 4. The best fit line to observed SII September SIE has a slope of -0.83 × 106 km2/decade. The models with the nearest trend are MPI-ESM-1-2-HR and MRI-ESM2-0 – both having a rate of -

0.72 × 106 km2/decade. All models except for CESM2-WACCM underpredict the rate of sea ice decline for this period – a trait previously observed common to most climate models (SIMIP Community, 2020).

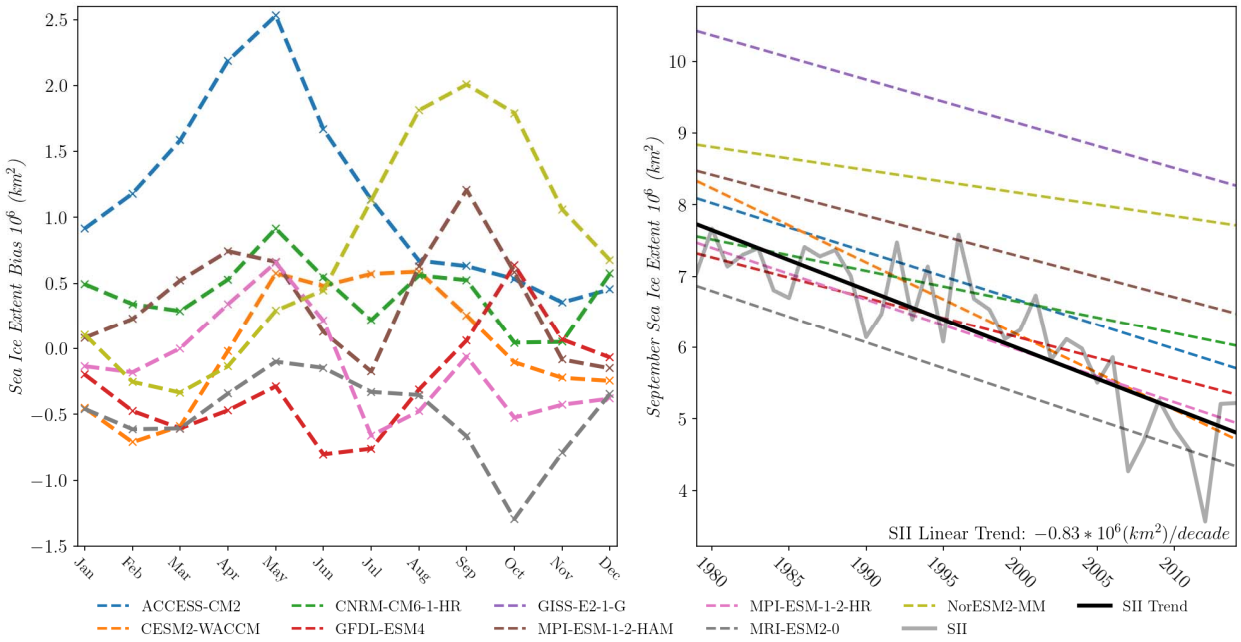

Figure 4. Average monthly SIE bias for each climate model over the period 1979 – 2014. (b): Observed and simulated September SIE linear trend compared to the NSIDC record. GISS-E2-1-G is not shown in the plot (a), as error for this model exceeds +2.5 × 106 km2 for all months.

Table 5. Monthly percent error in comparison to the NSIDC observations and September SIE linear trend (106 km2/decade) through the period 1979 – 2014.

MODEL:	ACCESS-CM2	CESM2-WACCM	CNRM-CM6-1-HR	GFDL-ESM4	GISS-E2-1-G	MPI-ESM-1-2-HAM	MPI-ESM-1-2-HR	MRI-ESM2-0	NorESM 2-MM
March Percent Error	10%	-4%	2%	-4%	35%	3%	0.0%	-4%	-2%
September Percent Error	10%	4%	8%	1%	49%	19%	-1%	-11%	32%
Annual Percent Error	10%	1%	4%	-2%	40%	4%	-2%	-5%	9%
Mean Absolute % Error	9.8%	3.7%	3.9%	3.6%	39.7%	4.6%	3.3%	5.1%	9.9%
September SIE Linear Trend ($10^6 km^2$/decade)	-0.68	-1.03	-0.44	-0.57	-0.62	-0.57	-0.72	-0.72	-0.32

3.4 Suface Air Temperature

The summary statistics derived from SAT analysis are presented in Table 5. Here, correlation coefficients are omitted from the statistical measure, as all models maintain annual correlation ≥0.97 when compared with ERA5 data. Examining mean error, all models except for MRI-ESM2-0 have negative annual bias. As previously mentioned, this is most likely driven by a previously acknowledged positive bias in ERA5 Arctic temperatures during the coldest winter

328 months and further evidenced by the large negative mean bias values for the month of the March
329 shown in Table 5. Considering the potential effect this bias may have during colder months,
330 assessment should prioritize September SAT performance where the ERA5 negative bias is not
331 present and climate model mean bias values are more evenly distributed.
332

333 **Table 6. Summary statistics for each climate model's surface air temperature in Celsius**
334 **(°C) compared with ERA5 monthly surface air temperature within the region from 1979 -**
335 **2014.**

Model	ACCESS-CM2	CESM2-WACCM	CNRM-CM6-1-HR	GFDL-ESM4	GISS-E2-1-G	MPI-ESM-1-2-HAM	MPI-ESM-1-2-HR	MRI-ESM2-0	NorESM 2-MM
SEPTEMBER									
RMSE	2.5	1.5	1.7	1.2	4.1	2.4	1.0	1.6	1.6
MEAN BIAS	-2.2	0.6	-1.2	0.7	-3.9	-2.0	-0.1	1.4	-1.2
MARCH									
RMSE	7.2	3.0	6.6	6.1	8.7	5.8	2.4	1.6	5.8
MEAN BIAS	-6.8	-2.0	-5.9	-5.2	-7.8	-5.0	-1.7	-0.4	-5.3
ANNUAL									
RMSE	5.1	2.2	4.7	3.9	5.8	3.8	1.9	1.9	4.4
MEAN BIAS	-4.1	-0.8	-3.7	-2.4	-4.8	-2.9	-0.6	0.2	-3.5

336 Temperature bias contour maps for the month of September can be seen in Figure 5. For
337 September, the model with the lowest RMSE and mean bias is MPI-ESM-1-2-HR at 1.0°C and
338 -0.1°C respectively. Examining the spatial bias of this model in Figure 5, it overestimates
339 temperature for most of the seas surrounding Greenland and within the Canadian Archipelago (a
340 feature observed in the majority of models) yet has minimal underestimation for the remainder of
341 the Arctic. CNRM-CM6-1-HR, GFDL-ESM4, MPI-ESM-1-2-HAM, MPI-ESM-1-2-HR, and
342 MRI-ESM2-0 all exhibit similar trends in high positive bias through the Canadian Archipelago,
343 Baffin Bay, and the Greenland Sea. GISS-E2-1G, ACCESS-CM2 and MPI-ESM-1-2-HAM have
344 consistent Pan-Arctic negative bias while ACCESS-CM2 and MPI-ESM-1-2-HAM also have
345 large areas of negative bias reaching from the North Pole through the East Siberian and into the
346 Bearing Sea. MRI-ESM2-0 has the lowest mean annual bias of 0.2°C and is even with MPI-
347 ESM-1-2-HR with the lowest annual RMSE of 1.9°C. Investigating this result, the model shows
348 minimal error during winter months (a result potentially driven by positive bias in ERA5 winter
349 temperatures and discussed in section 4) as shown for the month of March in Table 5. The
350 previously discussed SAT positive bias within ERA5 under extreme cold weather may have had
351 significant influence in this result and thus demand future investigation and confirmation.

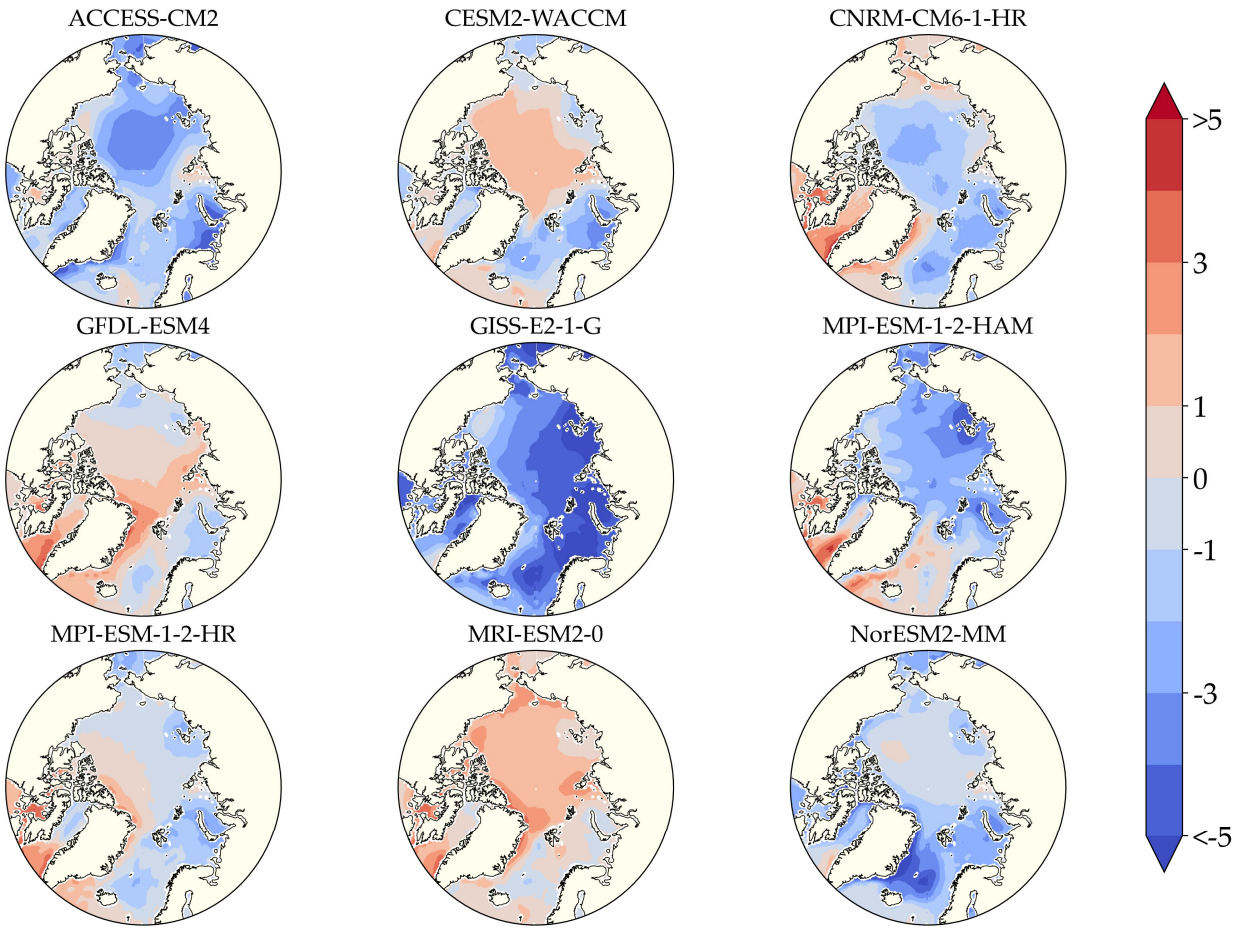

Figure 5. Surface air temperature bias for the month of September averaged over 1979-2014. Temperatures over land have been excluded from analysis and masked over for mapping.

3.5 Suface Wind Speed

Analysis of SWS yields the summary statistics shown in Table 6. The spread in annual RMSE between models is less than 0.7 m/s and the range in annual bias values does not exceed 2 m/s. MPI-ESM-1-2-HR maintains the lowest RMSE out of all the models for September, March, and annually. Most models (excepting NorESM2-MM) show improved correlation for March in comparison to September, with GFDL-ESM4 experiencing the largest improvement.

In Figure 6, the spatial bias contours can be used to elucidate the September statistics provided in Table 6. CNRM-CM6-1-HR and MRI-ESM2-0 immediately stand out as exhibiting pervasive positive bias for not only oceanic regions but also within coastal areas. A common feature in many of the models shown is a tendency for coastal areas to have considerable negative bias. This can be observed for the majority of models in the Beaufort Sea or along the southeast coast of Greenland. MPI-ESM-1-2-HR shows noticeably little bias exceeding 0.5m/s, demonstrating the accuracy of the model.

Table 7. Summary statistics for each climate model's surface wind speed simulation with ERA-5 monthly surface wind speed within the region north of 60°N from 1979 to 2014. RMSE and mean bias have units of m/s.

MODEL	ACCESS-CM2	CESM2-WACCM	CNRM-CM6-1-HR	GFDL-ESM4	GISS-E2-1-G	MPI-ESM-1-2-HAM	MPI-ESM-1-2-HR	MRI-ESM2-0	NorESM 2-MM
SEPTEMBER									
RMSE	0.79	0.33	0.68	0.63	0.49	0.70	0.29	1.02	0.51
MEAN BIAS	-0.63	-0.08	0.62	0.35	-0.24	-0.60	-0.05	0.99	-0.41
R	0.90	0.93	0.93	0.75	0.84	0.91	0.93	0.95	0.95
MARCH									
RMSE	0.69	0.68	0.46	0.51	0.74	0.57	0.44	1.27	1.03
MEAN BIAS	-0.40	-0.42	0.21	0.13	-0.37	-0.40	-0.19	1.22	-0.92
R	0.91	0.94	0.96	0.93	0.88	0.96	0.96	0.97	0.95
ANNUAL									
RMSE	0.75	0.63	0.56	0.54	0.62	0.69	0.41	1.07	0.94
MEAN BIAS	-0.51	-0.39	0.37	0.13	-0.23	-0.54	-0.16	0.99	-0.73
R	0.90	0.93	0.94	0.90	0.88	0.95	0.95	0.96	0.89

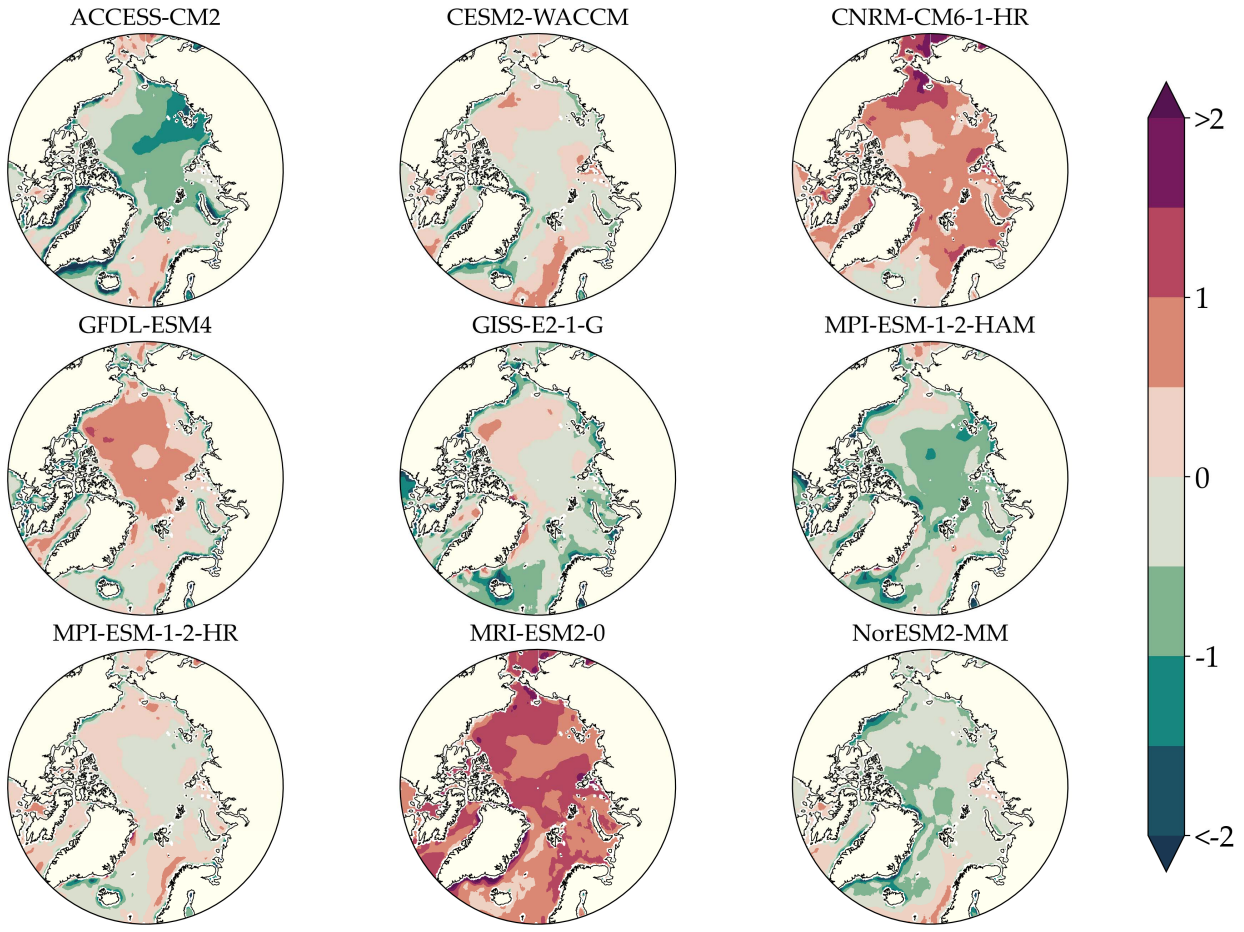

Figure 6. Monthly surface wind speed bias averaged for all months 1979 through 2014. Only surface winds corresponding to oceanic grid cells were considered for analysis.

4 Discussion and Conclusion

Assessment of climate model historical simulation of SIT shows that the spatial distribution diverges greatly between models. Mean annual SIT bias derived from comparison to

PIOMAS ranges from -0.63m to 1.11m and the comparison from CS2SMOS yields winter SIT bias ranging from -0.2m to 0.81m. Models have improved spatial correlation with PIOMAS over CS2SMOS; these results are partially expected, as PIOMAS shares several regions of inaccurate simulated SIT common to the climate models (J. Stroeve et al., 2014). Yet this may also stem from the brevity of the CS2SMOS time series used to establish the mean monthly SIT distribution and the inclusion of the anomalous 2012 September sea ice minimum. Despite the considerable inter-model variance observed, there are several trends common to the majority of models. Foremost, many of the models that otherwise show minimal error throughout most of the Arctic, fail to simulate the thickest sea ice regimes at the Lincoln Sea and extending towards north of the Canadian Archipelago. This strong negative bias (≤-1m) is present year-round for more than half the models. Notably, however, this bias is reduced for CS2SMOS in comparison to PIOMAS; suggesting that the models are perhaps more capable of simulating thinner ice (more sensitive to climate and oceanic forcing (Overland, 2020)) in the latter part of the time series.

Examining SIE simulation skill, all models are capable of simulating the basic features of the seasonal cycle, with maximum extent occurring in March and the minimum occurring in September. Most models exhibit positive bias for September and reduced error for March. Examining trends in September SIE, all models except for one (CESM2-WACCM) underestimate the rate of sea ice decline by at least 0.1 km2/decade. Both these results are in agreement with other studies showing that CMIP6 climate models generally underestimate the rate of sea ice retreat and struggle to capture the annual sea ice minimum. The MPI-ESM-1-2-HR ensemble average has very little bias for September mean SIE, the lowest annual absolute mean percentage error, and a comparable September SIE trend through the time series.

SAT comparison between climate models and ERA5 shows that nearly all models have an annual cold bias. This result is believed to have been driven by a warm bias present in the ERA5 dataset used in climate model assessment. Several studies have confirmed that ERA5 or ERA-Interim (predecessor to ERA5) possesses a sizeable Arctic SAT warm bias (+3.9°C to +5.4°C) during the winter months in extreme cold weather conditions (Demchev et al., 2020; Graham et al., 2019; C. Wang et al., 2019). The exact spatial and temporal characteristics of this warm bias are unclear and thus cannot be corrected; yet it is clear that the warm bias grows as air temperatures become colder, peaking in winter months at high latitudes. For this reason, emphasis in assessment should be placed on warmer months, such as the metrics derived for September. For September, the range of bias spans from -3.9°C to 1.4°C for the models GISS-E2-1-G and MRI-ESM2-0 respectively. For March, the inter-model bias ranges from -0.4°C to -7.8°C – yet the significance of these results are questionable given the acknowledged ERA5 bias. It is recommended that an alternative data source be used for SAT analysis in future analysis. Multiple atmospheric reanalysis products have been shown to possess a similar warm bias during extreme cold temperatures (Graham et al., 2019); however, this trend is especially pertinent in ERA5. Otherwise, the use of in situ data could be considered for comparison at the cost of losing spatial coverage and continuous data availability. Model simulations of wind show that most models have reliably high correlation values and annual bias not exceeding 1m/s. Most models commonly underestimate SWS in coastal areas and only two models exhibit a pervasive positive bias. MPI-ESM-1-2-HR has the lowest RMSE through all seasons and the highest annual correlation.

Climate model simulation of historical Arctic sea ice thickness, extent, surface wind speed, and temperature were analyzed against satellite, sea ice reanalysis, and atmospheric reanalysis data to derive skill metric statistic and bias contour maps. Coupled climate models represent an invaluable source of future climate data for regional modeling and research efforts. Individual climate models participating within CMIP6 may diverge substantially in ability to simulate historical sea ice and related climate variables, thus contributing to the uncertainty in projecting the future sea ice decline. By this rational, the evaluation and understanding of individual model historical simulation is desirable. Models were shown to present considerable differences in simulating the spatial distribution of SIT within the Arctic and no one model could be identified as presenting a totally resolved sea ice distribution representing observed conditions. Nonetheless, results and conclusions of this study contribute to the body of knowledge of climate model performance and may be used to inform model selection for reliant Arctic research. In comparison to CS2SMOS satellite data, MPI-ESM-1-2-HR led in all performance metrics overall and presented competitive performance in comparison to PIOMAS. For SAT, MRI-ESM2-0 presents the lowest annual mean bias and RMSE; however, this result is contentious due to a strong warm bias within the ERA5 data for winter months. Considering the rapid climate change in the Arctic, the ability to accurately predict the evolution and decline of sea ice within this region is crucial to predicting the timeline and scope of effects that will be felt worldwide. The findings in this study are presented with the intention of aiding regional Arctic research reliant on climate model forecasting data.

Acknowledgments

This material is based upon work supported by the National Science Foundation under Grant No. # 1927785. This funding is gratefully acknowledged but implies no endorsement of the findings. The authors would also like to thank NSF for the scholarships to the first, fourth, and fifth authors

Open Research

The climate model data from the World Climate Research Programme used within this study is freely available at: https://esgf-node.llnl.gov/projects/cmip6/ . Merged CryoSat-2/SMOS sea ice thickness is accessible via https://spaces.awi.de/display/CS2SMOS and PIOMAS sea ice thickness can be accessed through http://psc.apl.uw.edu/data/ . ERA5 surface wind speed and air temperature are available at https://cds.climate.copernicus.eu/ .

References

Aksenov, Y., Popova, E. E., Yool, A., Nurser, A. J. G., Williams, T. D., Bertino, L., & Bergh, J. (2017). On the future navigability of Arctic sea routes: High-resolution projections of the Arctic Ocean and sea ice. Marine Policy, 75, 300–317. https://doi.org/10.1016/j.marpol.2015.12.027

Barnhart, K. R., Overeem, I., & Anderson, R. S. (2014). The effect of changing sea ice on the physical vulnerability of Arctic coasts. Cryosphere, 8(5), 1777–1799. https://doi.org/10.5194/tc-8-1777-2014

Casas-Prat, M., Wang, X. L., & Swart, N. (2018). CMIP5-based global wave climate projections including the entire Arctic Ocean. Ocean Modelling, 123(January), 66–85. https://doi.org/10.1016/j.ocemod.2017.12.003

Casas-Prat, Mercè, & Wang, X. L. (2020). Sea Ice Retreat Contributes to Projected Increases in Extreme Arctic Ocean Surface Waves. Geophysical Research Letters, 47(15). https://doi.org/10.1029/2020GL088100

Chen, J., Kang, S., Chen, C., You, Q., Du, W., Xu, M., Zhong, X., Zhang, W., & Jizu, C. (2020). Changes in sea ice and future accessibility along the Arctic Northeast Passage. Global and Planetary Change, 195, 103319. https://doi.org/10.1016/j.gloplacha.2020.103319

Davy, R., & Outten, S. (2020). The arctic surface climate in CMIP6: Status and developments since CMIP5. Journal of Climate, 33(18), 8047–8068. https://doi.org/10.1175/JCLI-D-19-0990.1

Demchev, D. M., Kulakov, M. Y., Makshtas, A. P., Makhotina, I. A., Fil'chuk, K. V, & Frolov, I. E. (2020). Verification of ERA-Interim and ERA5 Reanalyses Data on Surface Air Temperature in the Arctic. Russian Meteorology and Hydrology, 45(11), 771–777.

Docquier, D., Grist, J. P., Roberts, M. J., Roberts, C. D., Semmler, T., Ponsoni, L., Massonnet, F., Sidorenko, D., Sein, D. V., Iovino, D., Bellucci, A., & Fichefet, T. (2019). Impact of model resolution on Arctic sea ice and North Atlantic Ocean heat transport. Climate Dynamics, 53(7–8), 4989–5017. https://doi.org/10.1007/s00382-019-04840-y

Docquier, D., & Koenigk, T. (2021). Observation-based selection of climate models projects Arctic ice-free summers around 2035. Communications Earth and Environment, 2(1), 1–8. https://doi.org/10.1038/s43247-021-00214-7

Doscher, R., Vihma, T., & Maksimovich, E. (2014). Recent advances in understanding the Arctic climate system state and change from a sea ice perspective: a review. Atmospheric Chemistry and Physics, 14(24), 13571–13600.

Goosse, H., Kay, J. E., Armour, K. C., Bodas-Salcedo, A., Chepfer, H., Docquier, D., Jonko, A., Kushner, P. J., Lecomte, O., Massonnet, F., Park, H. S., Pithan, F., Svensson, G., & Vancoppenolle, M. (2018). Quantifying climate feedbacks in polar regions. Nature Communications, 9(1). https://doi.org/10.1038/s41467-018-04173-0

Graham, R. M., Cohen, L., Ritzhaupt, N., Segger, B., Graversen, R. G., Rinke, A., Walden, V. P., Granskog, M. A., & Hudson, S. R. (2019). Evaluation of Six Atmospheric Reanalyses over Arctic Sea Ice from Winter to Early Summer. Journal of Climate, 32(14), 4121–4143.

Haine, T. W. N., Curry, B., Gerdes, R., Hansen, E., Karcher, M., Lee, C., Rudels, B., Spreen, G., de Steur, L., Stewart, K. D., & Woodgate, R. (2015). Arctic freshwater export: Status, mechanisms, and prospects. Global and Planetary Change, 125, 13–35. https://doi.org/10.1016/j.gloplacha.2014.11.013

Harsem, Ø., Heen, K., Rodrigues, J. M. P., & Vassdal, T. (2015). Oil exploration and sea ice projections in the Arctic. Polar Record, 51(1), 91–106.

Karlsson, J., & Svensson, G. (2013). Consequences of poor representation of Arctic sea-ice albedo and cloud-radiation interactions in the CMIP5 model ensemble. Geophysical Research Letters, 40(16). https://doi.org/10.1002/grl.50768

Knutti, R., Sedláček, J., Sanderson, B. M., Lorenz, R., Fischer, E. M., & Eyring, V. (2017). A climate model projection weighting scheme accounting for performance and interdependence. Geophysical Research Letters, 44(4), 1909–1918. https://doi.org/10.1002/2016GL072012

Kwok, R. (2018). Arctic sea ice thickness, volume, and multiyear ice coverage: Losses and coupled variability (1958-2018). In Environmental Research Letters (Vol. 13, Issue 10). Institute of Physics Publishing. https://doi.org/10.1088/1748-9326/aae3ec

Kwok, R., & Cunningham, G. F. (2015). Variability of arctic sea ice thickness and volume from CryoSat-2. Philosophical Transactions of the Royal Society A: Mathematical, Physical and Engineering Sciences, 373(2045). https://doi.org/10.1098/rsta.2014.0157

Kwok, R., Spreen, G., & Pang, S. (2013). Arctic sea ice circulation and drift speed: Decadal trends and ocean currents: ARCTIC SEA ICE MOTION. Journal of Geophysical Research. Oceans, 118(5), 2408–2425.

Laxon, S. W., Giles, K. A., Ridout, A. L., Wingham, D. J., Willatt, R., Cullen, R., Kwok, R., Schweiger, A., Zhang, J., Haas, C., Hendricks, S., Krishfield, R., Kurtz, N., Farrell, S., & Davidson, M. (2013). CryoSat-2 estimates of Arctic sea ice thickness and volume. Geophysical Research Letters, 40(4), 732–737. https://doi.org/10.1002/grl.50193

Lindsay, R., Wensnahan, M., Schweiger, A., & Zhang, J. (2014). Evaluation of seven different atmospheric reanalysis products in the arctic. Journal of Climate, 27(7), 2588–2606. https://doi.org/10.1175/JCLI-D-13-00014.1

Long, M., Zhang, L., Hu, S., & Qian, S. (2021). Multi-aspect assessment of cmip6 models for arctic sea ice simulation. Journal of Climate, 34(4), 1515–1529. https://doi.org/10.1175/JCLI-D-20-0522.1

Maslanik, J. A., Fowler, C., Stroeve, J., Drobot, S., Zwally, J., Yi, D., & Emery, W. (2007). A younger, thinner Arctic ice cover: Increased potential for rapid, extensive sea-ice loss. Geophysical Research Letters, 34(24), L24501-n/a.

552 Meier, W., Fetterer, F., Savoie, M., Mallory, S., Duerr, R., & Stroeve, J. (2017). NOAA/NSIDC
553 Climate Data Record of Passive Microwave Sea Ice Concentration. In Boulder, Colorado USA:
554 National Snow and Ice Data Center. https://doi.org/https://doi.org/10.7265/N59P2ZTG
555
556 Melia, N., Haines, K., & Hawkins, E. (2016). Sea ice decline and 21st century trans-Arctic
557 shipping routes. Geophysical Research Letters, 43(18), 9720–9728.
558
559 Mioduszewski, J., Vavrus, S., & Wang, M. (2018). Diminishing Arctic sea ice promotes stronger
560 surface winds. Journal of Climate, 31(19), 8101–8119. https://doi.org/10.1175/JCLI-D-18-
561 0109.1
562
563 Olason, E., & Notz, D. (2014). Drivers of variability in Arctic sea-ice drift speed. Journal of
564 Geophysical Research. Oceans, 119(9), 5755–5775.
565
566 Overland, J. E. (2020). Less climatic resilience in the Arctic. Weather and Climate Extremes, 30,
567 100275-.
568
569 Peng, G., Meier, W. N., Scott, D. J., & Savoie, M. H. (2013). A long-term and reproducible
570 passive microwave sea ice concentration data record for climate studies and monitoring. Earth
571 System Science Data, 5(2), 311–318. https://doi.org/10.5194/essd-5-311-2013
572

573 Ricker, R., Hendricks, S., Kaleschke, L., Tian-Kunze, X., King, J., & Haas, C. (2017). A weekly
574 Arctic sea-ice thickness data record from merged CryoSat-2 and SMOS satellite data. The
575 Cryosphere, 11(4), 1607–1623. https://doi.org/10.5194/tc-11-1607-2017
576
577 Schweiger, A. J., Steele, M., Zhang, J., Moore, G. W. K., & Laidre, K. L. (2021). Accelerated
578 sea ice loss in the Wandel Sea points to a change in the Arctic's Last Ice Area. Communications
579 Earth & Environment, 2(1), 1–12. https://doi.org/10.1038/s43247-021-00197-5
580
581 Schweiger, A., Lindsay, R., Zhang, J., Steele, M., Stern, H., & Kwok, R. (2011). Uncertainty in
582 modeled Arctic sea ice volume. Journal of Geophysical Research: Oceans, 116(9), 1–21.
583 https://doi.org/10.1029/2011JC007084
584
585 Shen, Z., Duan, A., Li, D., & Li, J. (2021). Assessment and ranking of climate models in Arctic
586 Sea ice cover simulation: From CMIP5 to CMIP6. Journal of Climate, 34(9), 3609–3627.
587 https://doi.org/10.1175/JCLI-D-20-0294.1
588
589 Shu, Q., Wang, Q., Song, Z., Qiao, F., Zhao, J., Chu, M., & Li, X. (2020). Assessment of Sea Ice
590 Extent in CMIP6 With Comparison to Observations and CMIP5. Geophysical Research Letters,
591 47(9). https://doi.org/10.1029/2020GL087965
592
593 Sibul, G., & Jin, J. G. (2021). Evaluating the feasibility of combined use of the Northern Sea
594 Route and the Suez Canal Route considering ice parameters. Transportation Research Part A:
595 Policy and Practice, 147(March), 350–369. https://doi.org/10.1016/j.tra.2021.03.024

SIMIP Community. (2020). Arctic Sea Ice in CMIP6. Geophysical Research Letters, 47(10). https://doi.org/10.1029/2019GL086749

Stroeve, J., Barrett, A., Serreze, M., & Schweiger, A. (2014). Using records from submarine, aircraft and satellites to evaluate climate model simulations of Arctic sea ice thickness. Cryosphere, 8(5), 1839–1854. https://doi.org/10.5194/tc-8-1839-2014

Stroeve, Julienne, & Notz, D. (2018). Changing state of Arctic sea ice across all seasons. In Environmental Research Letters (Vol. 13, Issue 10). Institute of Physics Publishing. https://doi.org/10.1088/1748-9326/aade56

Thomson, J., & Rogers, W. E. (2014). Swell and sea in the emerging Arctic Ocean. Geophysical Research Letters, 41(9), 3136–3140. https://doi.org/10.1002/2014GL059983

Timmermans, M. L., & Marshall, J. (2020). Understanding Arctic Ocean Circulation: A Review of Ocean Dynamics in a Changing Climate. Journal of Geophysical Research: Oceans, 125(4), 1–35. https://doi.org/10.1029/2018JC014378

Tschudi, M. A., Stroeve, J. C., & Stewart, J. S. (2016). Relating the Age of Arctic Sea Ice to its Thickness, as Measured during NASA's ICESat and IceBridge Campaigns. Remote Sensing (Basel, Switzerland), 8(6), 457.

Wang, C., Graham, R. M., Wang, K., Gerland, S., & Granskog, M. A. (2019). Comparison of ERA5 and ERA-Interim near-surface air temperature, snowfall and precipitation over Arctic sea ice: effects on sea ice thermodynamics and evolution. The Cryosphere, 13(6), 1661–1679. https://doi.org/10.5194/tc-13-1661-2019

Wang, X., Key, J., Kwok, R., & Zhang, J. (2016). Comparison of Arctic sea ice thickness from satellites, aircraft, and PIOMAS data. Remote Sensing, 8(9). https://doi.org/10.3390/rs8090713

Watts, M., Maslowski, W., Lee, Y. J., Kinney, J. C., & Osinski, R. (2021). A spatial evaluation of arctic Sea ice and regional limitations in CMIP6 historical simulations. Journal of Climate, 34(15), 6399–6420. https://doi.org/10.1175/JCLI-D-20-0491.1

Wei, T., Yan, Q., Qi, W., Ding, M., & Wang, C. (2020). Projections of Arctic sea ice conditions and shipping routes in the twenty-first century using CMIP6 forcing scenarios. Environmental Research Letters, 15(10).

Williams, D. M., & Erikson, L. H. (2021). Knowledge Gaps Update to the 2019 IPCC Special Report on the Ocean and Cryosphere: Prospects to Refine Coastal Flood Hazard Assessments and Adaptation Strategies With At-Risk Communities of Alaska. Frontiers in Climate, 3(December), 1–11. https://doi.org/10.3389/fclim.2021.761439

640 Zhang, J., & Rothrock, D. A. (2003). Modeling global sea ice with a thickness and enthalpy
641 distribution model in generalized curvilinear coordinates. Monthly Weather Review, 131(5),
642 845–861. https://doi.org/10.1175/1520-0493(2003)131<0845:MGSIWA>2.0.CO;2